AJNR

Scalloping deformity of the corpus callosum following ventricular shunting.

Y Numaguchi, D A Kristt, C Joy and W L Robinson

AJNR Am J Neuroradiol 1993, 14 (2) 355-362
http://www.ajnr.org/content/14/2/355

This information is current as of May 4, 2025.

Scalloping Deformity of the Corpus Callosum following Ventricular Shunting

Yuji Numaguchi,[4] Donald A. Kristt,[2] Christopher Joy,[1] and Walker L. Robinson[3]

PURPOSE: To describe six patients who underwent ventriculoperitoneal (V-P) shunting for hydrocephalus and developed scalloping deformity of the dorsal surface of the corpus callosum, and to evaluate the cause and frequency of this phenomenon. **MATERIALS AND METHODS:** MR images of 35 patients whose hydrocephalus was successfully corrected by V-P shunting were studied. To elucidate the possible anatomic basis for the scalloping deformity, gross examination of the corpus callosum relative to the adjacent anatomical structures was performed using autopsy specimens. **RESULTS:** Of the 35 patients who underwent successful V-P shunting, six (17%) developed a scalloping deformity of the corpus callosum. The deformity was noted exclusively in the body of the corpus callosum. This phenomenon was observed in both obstructive and communicating hydrocephalus regardless of the patient's age, but was particularly noted in patients with tectal tumors. **CONCLUSION:** The cause of this phenomenon may be a combination of long-standing hydrocephalus and normal pericallosal artery anatomy. Prolonged hydrocephalus softens the corpus callosum and the branches of the pericallosal arteries tether the corpus callosum to the overlying cingulate cortex at periodic intervals.

Index terms: Corpus callosum, abnormalities and anomalies; Shunts, complications; Hydrocephalus

AJNR 14:355–362, Mar/Apr 1993

Anatomical, embryologic, and pathologic abnormalities of the corpus callosum have been described in numerous reports. The advent of magnetic resonance (MR) imaging with its various pulse sequences has facilitated the diagnosis of such corpus callosum lesions, including anomalies, neoplasms, and posttraumatic and degenerative disorders (1–7).

Six patients underwent ventriculoperitoneal (V-P) shunting for hydrocephalus, and developed scalloping deformity of the corpus callosum associated with increased accumulation of cerebrospinal fluid (CSF) in the callosal sulcus. There is no previous description of this abnormality in the literature. The MR findings of these patients were analyzed in relation to gross anatomic examination of the corpus callosum and its vasculature which suggested possible pathogenetic mechanisms.

Patients and Methods

During the past 30 months, 282 patients underwent V-P shunting for hydrocephalus at our institution. Among them, 53 patients had postshunt MR imaging at various intervals. In 35 patients of the 53, their MR imaging demonstrated significant reduction of size of the ventricular system. Six of the 35 (17%) had scalloping deformity of the superior surface of the corpus callosum on sagittal T1-weighted images. The age range was 6 to 62 years (average, 29 years). There were four males and two females. Four patients had tumors of the tectal region: two astrocytomas, one glioblastoma multiforme, and one presumed glioma. One patient had communicating hydrocephalus with a diagnosis of normal pressure hydrocephalus. One patient had moderate hydrocephalus associated with Chiari I malformation and syringohydromyelia in the cervical region. All patients had moderate to marked hydrocephalus, documented by computed tomography (CT) and/or MR imaging. V-P shunting had been performed only once in three patients. Three patients had two or more shunt revisions prior to their initial MR examination. The V-P shunts were

Received November 7, 1990; revision requested January 9, 1992; final revision received February 20 and accepted February 24.

[1] Department of Radiology, [2] Neuropathology, and [3] Neurosurgery, University of Maryland Medical System, Baltimore, MD 21201.

[4] Address reprint requests to Yuji Numaguchi, MD, Neuroradiology, Diagnostic Radiology, University of Maryland Medical System, 22 S. Greene Street, Baltimore, MD 21201.

AJNR 13:355–362, Mar/Apr 1993 0195-6108/93/1402–0355

© American Society of Neuroradiology

placed in the frontal horn of the lateral ventricle unilaterally or bilaterally via a frontal approach in four patients, and through the atrium via temporooccipital approach in one patient. Four patients received external beam radiotherapy for their tectal tumors with total (tumor dose of 50–60 Gy during the 5–7 weeks postshunt). All patients had noncontrast CT scans within 2 weeks following V-P shunting.

All patients had MR imaging performed at 1.5 T (Magnetom, Siemens, Madison, WI). Sagittal 5-mm sections (1-mm gap) spin-echo (SE) T1-weighted images were obtained using parameters of 500–650/17–20/2 (TR/TE/excitation), at 256 × 256 or 256 × 192 acquisition matrix. Axial 5-mm (1-mm gap) SE images, 2,000–2,500/25–35,60–90/1, and additional coronal 5-mm SE images, 2,500/35,90/1 were obtained for four patients.

T1-weighted images using gadopentetate dimeglumine were obtained for all patients having tectal tumors. Gradient refocused imaging in the sagittal plane with a parameter of 16/19/10 (TR/TE/flip angle) was used for one patient (patient 1). The initial MR imaging was performed within 2 months following the V-P shunting in four patients and at 12 months in one patient. Follow-up MR imaging was obtained in four patients after intervals of 3 to 14 months following their initial MR studies.

Gross examination of the corpus callosum relative to the adjacent anatomical structures was performed using the autopsy specimens of one study patient (case 4) and three subjects who died of nonneurologic diseases to elucidate the possible anatomic basis for the scalloping deformity of the corpus callosum.

Results

Noncontrast CT scan following the last V-P shunting showed minimal to moderate reduction in size of the ventricular system in all patients. Universal dilation of the subarachnoid space including the callosal sulcus was also noted.

The patients' clinical and MR findings are summarized in Table 1.

Scalloping deformity of the corpus callosum was most striking in case 1 (Fig. 1). T1-weighted sagittal images showed the periodic trough-like depression or "scalloping" in the dorsal surface of the entire body of the corpus callosum. The genu and splenium were free of scalloping. T1-weighted sagittal images revealed decreased signal intensity in the genu and body of the corpus callosum. Indentations were also noted in the cingulate gyrus of this patient in sites corresponding to the "scalloped" corpus callosum. Extensive accumulation of CSF was observed in these indented spaces between the corpus callosum and the cingulate gyrus (in the callosal sulcus), especially over the body of the corpus callosum. Increased CSF accumulation was also noted in adjacent cisterns and sulci, including the cingulate sulcus, and the retropulvinar cisterns.

A less prominent scalloping deformity of the corpus callosum associated with minimal to moderate CSF accumulation in the callosal sulcus was noted in five other patients (cases 2–6). Scalloping on sagittal T1-weighted images appeared on axial images as parenchymal bands or raised folds of the corpus callosum traversing the CSF accumulation (Fig. 2). This was noted about the entire body of the corpus callosum in three patients, and focally in the body segment of two patients. Diffuse thinning or atrophy of the corpus callosum was observed in one patient (case 2). Decreased signal intensity in the corpus callosum seen in case 1 was noted focally in the body of cases 3 and 4.

Follow-up MR imaging was performed in four patients. After 3 months, there was significant improvement of the scalloping deformity and reduction of CSF accumulation in case 1. A second MR study was performed in case 1 13 months postshunt. Although the tectal tumor had not changed significantly in size and configuration, there was further improvement of the scalloping deformity of the corpus callosum. Previously noted generalized CSF space dilatation became less prominent. However, low signal intensity persisted throughout the entire body and there was focal thinning (atrophy) in the posterior portion of the body. Complete resolution of the scalloping deformity of the corpus callosum was noted in cases 3 and 4 after 14 and 3 months, respectively. One patient (case 2) who presented with presumed atrophy of the entire corpus callosum and minimal scalloping on initial MR study showed no appreciable change on MR after 10 months.

All patients had symptoms related to hydrocephalus: headaches, nausea and vomiting, or ataxia. These resolved after V-P shunting. The tectal tumor size and configuration did not change significantly in three of four patients during the period of this study. The tectal tumor demonstrated on MR in case 4 progressively increased in size. She died of massive tumoral hemorrhage after a follow-up MR study. Scalloping deformity and CSF accumulation in the callosal sulcus were no longer visualized in the follow-up MR study of this patient.

Anatomical Observations

The brain of one patient in this series (case 4) was evaluated at autopsy. No definite scalloping

TABLE 1: Summary of patients' findings

Case No.	Age (yr)	Sex	Diagnosis and Treatment	Interval from Last V-P Shunting until MR	MR Images of CC and Associated Findings	Follow-up MR Findings
1	6	M	Tectal tumor; V-P shunt and radiation therapy	1 week	Marked scalloping of entire body; diffusely decreased signal in the genu and body on T1W; large CSF accumulation in CS	After 3 months: significant improvement of scalloping and signal intensity of CC and reduction of CSF accumulation in CS After 13 months: further improvement of scalloping; localized atrophy in body; low intensity in entire body persisted; no change in tumor size
2	6	F	Astrocytoma in tectum; V-P shunt and radiation therapy	12 months	Moderate atrophy of CC and focal scalloping in anterior body; minimal CSF accumulation in CS	After 10 months: no change
3	9	M	Astrocytoma in tectum; partial resection and radiation therapy; two shunt revisions since age of 8 years	2 months	Minimal scalloping in entire body with localized decreased signal intensity on T1W; minimal CSF accumulation in CS	After 14 months: CC and CS became normal in appearance; no change in tumor size
4	62	F	Glioblastoma multiforme in tectum; V-P shunt and radiation therapy	3 weeks	Minimal scalloping in entire body with localized decreased signal intensity on T1W; minimal CSF accumulation in CS	After 3 months: CC and CS became normal in appearance; significant increase in tumor size
5	45	M	Communicating hydrocephalus; two shunt revisions since age of 44 years	1 month	Minimal to moderate scalloping in mid and posterior body; moderate CSF accumulation in CS	
6	46	F	Chiari malformation with syringohydromyelia; multiple V-P shunt revisions	13 months	Minimal scalloping in entire body, localized atrophy of body	

Note.—CC = corpus callosum; CS = callosal sulcus; T1W = T1-weighted images.

or indentations in the surface of the corpus callosum including the indusium griseum was noted in this case. Microscopic evaluation of the corpus callosum including the use of myelin stains did not provide any indication of demyelination in the corpus callosum.

The anatomical relationship between the corpus callosum, cingulate gyrus, and pericallosal artery, including its branches, was also studied using the autopsy specimens of three other subjects who died of nonneurologic diseases. Multiple small pial branches from the pericallosal artery were observed to firmly anchor the pericallosal artery to the cingulate cortex. The pericallosal artery was noted loosely attached to the corpus callosum, except at points where the perforating medullary arterial branches of the pericallosal artery (8, 9) were found to vertically penetrate the corpus callosum at intervals (Fig. 3A). These perforating branches were also seen on sagittal sections examined microscopically and ran vertically from the dorsal surface of the corpus callosum toward the ventral surface. Tiny arterial twigs from the pericallosal artery were also noted to run laterally on the surface of the corpus callosum at intervals to supply both the corpus callosum and cingulate gyrus (Fig. 3B). These transverse pericallosal twigs represent the "pericallosal mustache" observed on carotid angio-

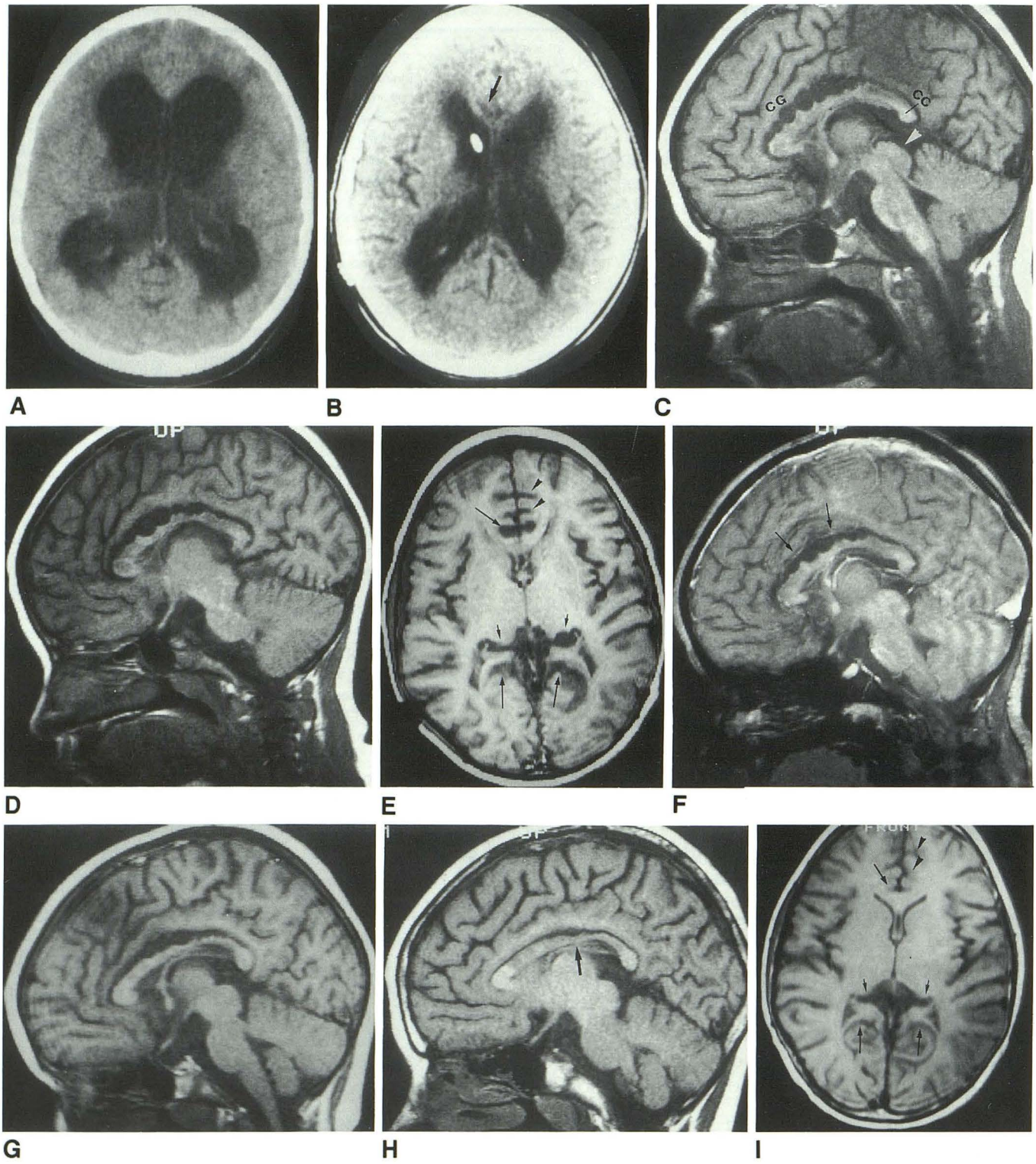

Fig. 1. Case 1.

A and *B*, CT before and 3 days after V-P shunting. Moderate resolution of hydrocephalus after shunting is noted. There is universal dilatation of the subarachnoid space including the sylvian fissures and callosal sulcus (*arrow*). The shunt tube tip terminates in the right frontal horn.

C and *D*, Contiguous sagittal T1-weighted MR images 1 week after shunting reveal a tectal mass (*arrowhead*) producing aqueductal stenosis. There is unusual scalloping deformity of the body of the corpus callosum (*CC*) and cingulate gyrus (*CG*) associated with CSF accumulation in the callosal sulcus. The entire corpus callosum except for the splenium has a decreased signal intensity which is well shown in *D*.

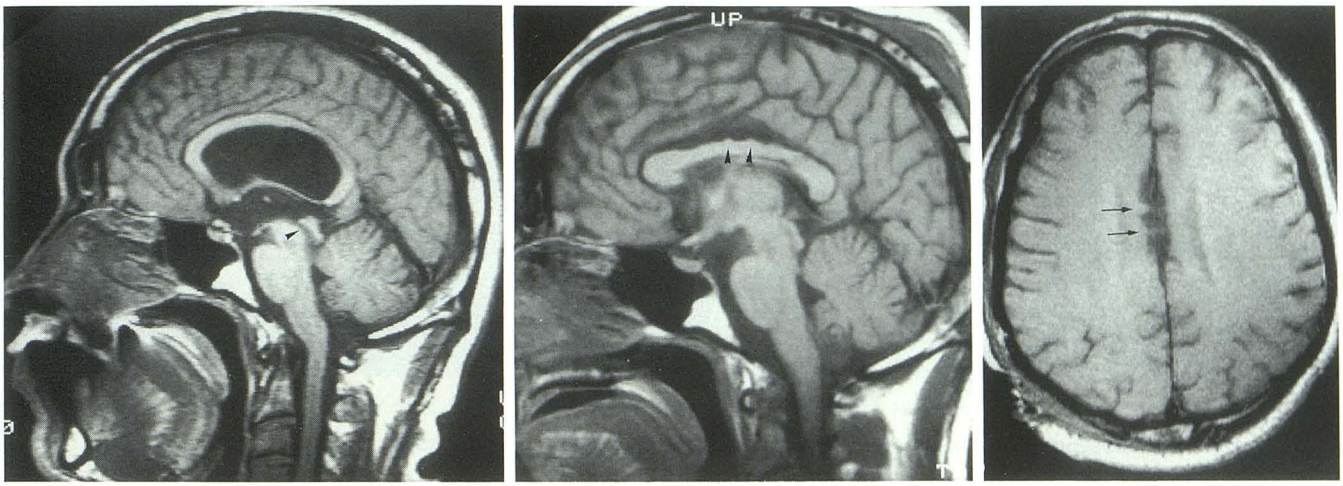

Fig. 2. Case 5.

A, Sagittal T1-weighted image shows moderate hydrocephalus with stretched corpus callosum. The aqueduct is patent (*arrowhead*).

B, Sagittal T1-weighted image obtained 1 month after V-P shunting demonstrates scalloping deformity on the corpus callosum (*arrowheads*), especially those involving the body, associated with CSF accumulation in the callosal sulcus.

C, Axial T1-weighted image through the expanded callosal sulcus demonstrates parenchymal bands or raised folds of the corpus callosum traversing the CSF accumulation (*arrows*).

grams when these twigs are superimposed on anterioposterior projections (8).

Prevalence of Scalloping Deformity

The six patients reported here were among 35 patients with MR demonstration of successful decompression of hydrocephalus by ventricular shunting. The cause of hydrocephalus and their ages are shown in Table 2. Typical scalloping deformity of the superior surface of the corpus callosum was most frequently observed in four of the seven patients with tectal tumors. All of them had severe hydrocephalus prior to ventricular shunting. This deformity was found in one of the two patients with hydrocephalus associated with syringohydromeylia, and in one of eight patients with communicating hydrocephalus of various etiologies. In none of the eight patients with posterior fossa masses, six patients with supratentorial tumors, and four patients with idiopathic aqueductal stenosis, scalloping deformity was visualized on postshunt MR imaging.

We analyzed the difference in occurrence of the scalloping deformity among disease groups using the Student *t* test. Simple correlation analysis was performed between age and occurrence of scalloping. The *t* test proved a significantly higher occurrence of scalloping deformity in patients with tectal tumors compared to the patients with other etiologies ($P = .001$). However, no significant correlation was observed between the patient's age and occurrence of scalloping.

Discussion

The scalloping deformity of the corpus callosum and its pathophysiology are not described in the literature. Schellinger et al (10) and Palmieri et al (11) did not describe corpus callosum abnormality in their extensive evaluation of the CT

E, T1-weighted axial image shows universally increased CSF space including the callosal sulcus (*long arrows*), retropulvinar cisterns (*short arrows*), and cingulate and frontal sulci (*arrowheads*).*F*, A gradient-echo image shows the pericallosal artery (*arrows*) situated above the CSF accumulation and along the cingulate gyrus, not immediately above the corpus callosum.

G, T1-weighted sagittal image, 3 months postshunting. Reduced scalloping deformity of the corpus callosum is noted associated with decreasing CSF accumulation in the callosal sulcus.

H and *I*, Sagittal and axial T1-weighted images, 13 months postshunting. Scalloping deformity has nearly resolved. Localized thinning of the body may represent atrophy (*thick arrow*). Low intensity in the entire body persisted. Generalized CSF space dilatation is still visualized but less prominent compared to *E*, especially in the callosal sulcus (*long arrows*), retropulvinar cistern (*short arrow*), and cingulate and frontal sulci (*arrowheads*).

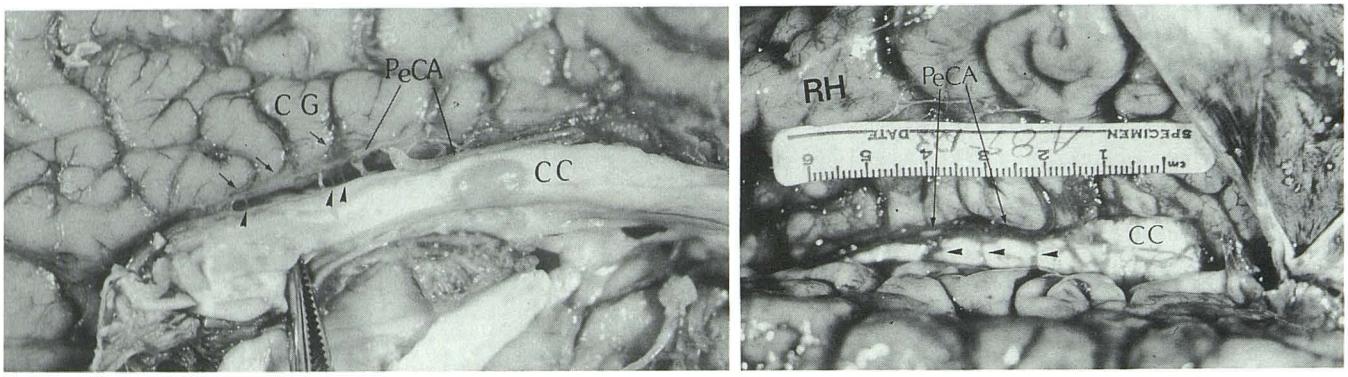

A B

Fig. 3. Anatomical observation of the corpus callosum and adjacent structures in the autopsy specimen of one subject, not related to the present series.

A, The parasagittal view demonstrating the corpus callosum (*CC*), cingulate gyrus (*CG*), and pericallosal artery (*PeCA*). Small arteries representing the perforating medullary arteries penetrate the corpus callosum (*arrowheads*) and the pial branches of the pericallosal artery firmly anchor the cingulate gyrus (*arrows*).

B, View of the callosal sulcus from above demonstrates the transverse pericallosal twigs that derive from the pericallosal artery and run laterally over the dorsal surface of the corpus callosum at intervals (*arrowheads*). *RH*-medial surface of right hemisphere.

TABLE 2: Causes of hydrocephalus and scalloping deformity of the corpus callosum

	No. of Patients with Scalloping Deformity	Patient's Age
Tectal tumor (n = 7)	4	6, 6, 9, 10, 27, 46, 62
Idiopathic aqueductal stenosis (n = 4)	0	8, 10, 11, 13
Posterior fossa tumor or cyst (n = 8)	0	1, 5, 7, 11, 13, 16, 30, 58
Supratentorial tumor or cyst (n = 6)	0	6, 8, 12, 33, 41, 63
Syringohydromyelia (n = 2)	1	12, 47
Communicating hydro (n = 8)	1	8, 15, 25, 25, 45, 62, 63, 82

Note.—The ages underlined represent patients with scalloping.

findings of hydrocephalic patients after ventricular shunting.

Several factors are likely to contribute to the development of this phenomenon. One is presumed softening of the body of the corpus callosum suggested by the areas of decreased signal intensity of the corpus callosum on the T1-weighted images of our three patients. Decreased signal intensity suggests edema, ischemia, and/or loss of myelinated fibers. These pathologic changes could result from prolonged severe stretching of the corpus callosum (12–14) (Fig. 4A). The corpus callosum would be expected to collapse ventrally as a result of the reduced pressure on the ventral surface when the hydrocephalus is treated (Fig. 4B). The peaks occurring periodically between the troughs suggest that tethering does occur and that the vascular network of the callosal sulcus described above serves as an anatomic substrate. Our normal gross specimens and previous anatomical studies (8, 9) demonstrate that the corpus callosum is tethered at intervals corresponding to the locations of the major rami of the pericallosal artery: namely, the pial arteries of the cingulate gyrus and perforating medullary arteries of the corpus callosum and transverse pericallosal twigs that supply the corpus callosum and cingulate gyrus (Fig. 3). The pericallosal artery appears more tightly tethered along the horizontal course to the cingulate gyrus than the body of the corpus callosum. This hypothesis is applicable to case 1 whose sagittal gradient-echo images demonstrated the pericallosal artery situated above the CSF accumulation along the cingulate cortex, not immediately above the corpus callosum (Fig. 1F).

Accumulation of CSF in the callosal sulcus apparently represented part of the increased CSF reservoir commonly occurring in the subarachnoid space as a direct result of alleviating long-standing hydrocephalus (10).

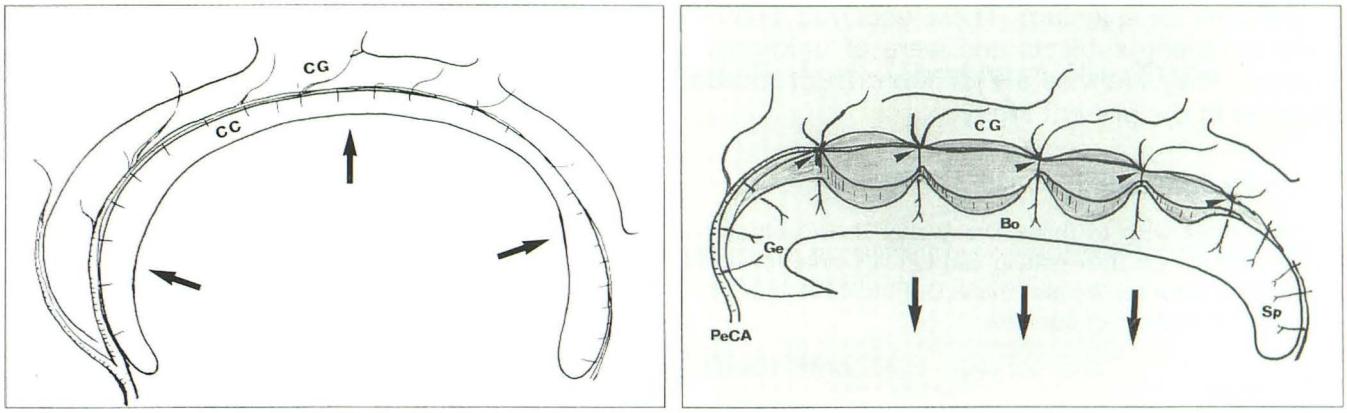

Fig. 4. A hypothesis to explain the mechanism of development of scalloping deformity of the corpus callosum, associated with CSF accumulation in the callosal sulcus.

A, The corpus callosum (*CC*) and cingulate gyrus (*CG*) accompanied by the pericallosal artery (*PeCA*) and its branches, are stretched and reduced in thickness due to ventriculomegaly as indicated by arrows.

B, Conditions immediately following correction of hydrocephalus by ventricular shunting. The corpus callosum, particularly the body segment (*Bo*) is relaxed and sags inferiorly as indicated by *arrows* but does not assume its original shape because of its lessened consistency. The corpus callosum and cingulate gyrus (*CG*) are tethered at intervals corresponding to the sites of the arterial rami of the pericallosal artery (*PeCA*) which vascularize these structures (*arrowheads*). The undulating configuration of alternating peaks and valleys producing the characteristic "scalloped" appearance of the corpus callosum is due to segmental collapse of the corpus callosum between these points of tethering. Scalloping deformity is not visualized in the genu (*Ge*) and splenium (*Sp*) because the pericallosal artery relate vertically with these segments of the corpus callosum and tethering does not occur.

The scalloping deformity was specifically limited to the body. The genu and the splenium were not involved. This supports the tethering theory because the geometry of the genu and the splenium would not permit a ventrally-directed concavity to develop, even though radiologic changes such as decreased signal intensity in the substance of the callosum similar to those occurring in the body are also present (Fig. 1D).

The development of the scalloping deformity of the corpus callosum may be determined by the duration and severity of the hydrocephalus. Hydrocephalus, moderate to marked of short duration or corrected rapidly, probably does not cause scalloping. This hypothesis is supported by the fact that four of our six patients presumably had long-standing severe obstructive hydrocephalus due to tectal tumors. The scalloping deformity will probably be best demonstrated relatively early, within a few months following ventricular shunting as seen in case 1. Disappearance or resolution of scalloping deformity was noted in three of our four patients during follow-up MR imaging performed at intervals of 3 to 14 months. This was probably due to gradual absorption of CSF from the callosal sulcus and reconstitution of the internal structures of the corpus callosum.

Diffuse or focal low intensity in the corpus callosum noted on T1-weighted images in three patients probably indicate edema and/or paucity of myelinated fibers and their replacement by numerous reactive astrocytes as described by Rubin et al (12). This low density disappeared or became less distinct on follow-up MR images indicating that such pathologic conditions created by hydrocephalus will be reversible (13). However, irreversible structural damage such as atrophy of the corpus callosum as noted in three patients can occur as a result of long-term stretching of the corpus callosum (5, 12). Such structural damage of the corpus callosum can also occur due to degeneration of the hemispheric axons as a consequence of long-standing ventricular dilatation (15, 16).

It is well known that focal thinning of the corpus callosum occurs at the junction of the body and the splenium in normal subjects (2, 17). Okamoto et al recently described a focal indentation at the anterior portion of the body of the corpus callosum in the normal subject, presumably due to the impression of the pericallosal artery (18). We have occasionally observed this vascular indentation on MR. Scalloping deformities of the corpus callosum described in this report are apparently different from such normal indentations. Roessmann and Friede (19) once described minimal indentations on the surface of the corpus callosum which were distributed from

the genu to the splenium. These occurred exclusively in elderly subjects and were of unknown etiology. They likewise are different from those observed in the present study.

Acknowledgments

The authors wish to thank Drs Walter J. Russell and Paul H. Pevsner for their editing and Linda Clarke for her secretarial assistance. We also thank Dr Futoshi Mihara for his statistical analysis of our data.

References

1. Simon JH, Holtas SL, Schiffer RB, et al. Corpus callosum and subcallosal-periventricular lesions in multiple sclerosis: detection with MR. *Radiology* 1986;160:363–367
2. McLeod NA, Williams JP, Machen B, Lum GB. Normal and abnormal morphology of the corpus callosum. *Neurology* 1987;37:1240–1242
3. Barkovich AJ, Norman D. Anomalies of the corpus callosum: correlation with further anomalies of the brain. *AJNR* 1988;9:493–501
4. Reinarz SJ, Coffman CE, Smoker WRK, Godersky JC. MR imaging of the corpus callosum: normal and pathologic findings and correlation with CT. *AJNR* 1988;9:649–656
5. Njiokiktjien C, Valk J, Ramaekers G. Malformation or damage of the corpus callosum? A clinical and MRI study. *Brain Dev* 1988; 10:92–99
6. Gentry LR, Thompson B, Godersky JC. Trauma to the corpus callosum: MR features. *AJNR* 1988;9:1129–1138
7. Jinkins JR, Whitemore AR, Bradley WG. MR imaging of callosal and corticocallosal dysgenesis. *AJNR* 1989;10:339–344
8. Huang YP, Wolf BS. Angiographic features of the pericallosal cistern. *Radiology* 1964;82:14–23
9. Moody DM, Bell MA, Challa VR. The corpus callosum, a unique white matter tract: anatomic features that may explain sparing in Binswanger disease and resistance to flow of fluid masses. *AJNR* 1988;9: 1051–1059
10. Schellinger D, McLough DC, Pederson RT. Computed tomography in the hydrocephalic patient after shunting. *Radiology* 1980;137: 693–704
11. Palmieri A, del Vecchio E, Ambrosio A, Pasquini U, Menichelli F, Salvolini U. Immediate and late effect of ventricular shunting. *Neurosurgery* 1982;23:203–205
12. Rubin RC, Hochwald GM, Tiell M, Epstein F, Ghatak N, Wisnieski H. Hydrocephalus. III. Reconstitution of the cerebral cortical mantle following ventricular shunting. *Surg Neurol* 1976;5:179–183
13. Gadsdon DR, Variend S, Emery JL. Myelination of the corpus callosum. II. The effect of relief of hydrocephalus upon the process of myelination. *Z Kinderchir* 1979;28:314–321
14. Del Bigio MR, Bruni JE. Changes in periventricular vasculature of rabbit brain following induction of hydrocephalus and after shunting. *J Neurosurg* 1988;69:115–120
15. Jinkins JR. Clinical manifestations of hydrocephalus caused by impingement of the corpus callosum on the falx: an MR study in 40 patients. *AJNR* 1991;12:331–340
16. Benzel EC, Pelletier AL, Levy PG. Communicating hydrocephalus in adults: prediction of outcome after ventricular shunting procedures. *Neurosurgery* 1990;26:655–660
17. Barkovich AJ, Kjos BO. Normal postnatal development of the corpus callosum as demonstrated by MR imaging. *AJNR* 1988;9:487–491
18. Okamoto K, Ito J, Tokiguchi S. The MR findings of the corpus callosum of normal young volunteers. *Nippon Acta Radiol* 1990;50:954–963
19. Roessmann J, Friede RL. Surface lesions of corpus callosum. *Acta Neuropathol* 1968;10:151–158